Functional modification of poly(vinyl alcohol) by copolymerizing with a hydrophobic cationic double alkyl-substituted monomer

Jiaojiao Ma, Xiande Yin, Hongqin Xiao, Ying Li, Jianjun Bao

State Key Laboratory of Polymer Materials Engineering, Polymer Research Institute, Sichuan University, Chengdu 610065, China
Correspondence to: J. Bao (E-mail: jjbao2000@sina.com)

ABSTRACT: In this paper, a hydrophobic monomer (HM) that has a cationic double alkyl-substituted group bonded to the nitrogen atom was first synthesized. Then a hydrophobic poly(vinyl alcohol) (PVA) was prepared by a radical solution copolymerization of vinyl acetate (VAc) with the HM followed by an alcoholysis reaction in alkaline conditions. The structures of HM and hydrophobically modified PVA (H-PVA) were confirmed by Fourier transform infrared spectroscopy and nuclear magnetic resonance. The effect of hydrophobic cationic segments on crystallization behaviors, mechanical properties, morphology, solution viscosity, and hydrophobic property were investigated. The results indicated that the crystallinity decreased from 37.2% of pure PVA to the minimum 23.2% of H-PVA with the incorporation of 1.15 mol % HM. The thermal decomposition temperature of H-PVA increased by about 50 °C compared with that of pure PVA. The viscosity of the H-PVA solution was several times higher than that of the corresponding unmodified PVA solution over the whole shear rate range, which demonstrated that the H-PVA had good shear-resistance ability. Furthermore, the contact angle was significantly increased from 55.1° to 115° with the incorporation of only 0.83% HM, which illustrated that the H-PVA had high hydrophobicity. © 2016 Wiley Periodicals, Inc. J. Appl. Polym. Sci. **2016**, *133*, 43888.

INTRODUCTION

Poly(vinyl alcohol) (PVA), prepared from hydrolysis of poly(vinyl acetate) (PVAc), is a water-soluble polymer with great film-formation and adhesive properties and excellent biocompatibility, biodegradability, and nontoxicity.[1–4] Therefore, PVA has been widely used in the fields of fibers, coatings, paper adhesives, emulsifiers, oil chemicals, drug slow-release systems, and so on.[5–7] Unfortunately, conventional PVA suffers from many drawbacks, such as poor water resistance, weak mechanical strength, low shear-resistance ability, and a narrow thermal processing window, extremely limiting its industrial applications. Therefore, hydrophobic modification of PVA to overcome these drawbacks is urgently needed.[8–10]

Recently, hydrophobically modified PVA (H-PVA) with a small number of pendant hydrophobes distributed along the backbone has attracted appreciable interest because of the potential commercial applications as oil-displacement agent, fluid-loss additive, and paper-sizing agent.[11,12] For example, when H-PVA is applied to a paper surface, the hydrophilic groups arrange inward and interact with the wood pulp fibers to form hydrogen bonds or chemical bonds and subsequently adhere firmly to the surface of the paper to enhance the strength of paper products. The hydrophobic groups arrange outward to resist the entrance of water molecules from the outside, which can greatly improve its water fastness. In addition, the hydrophobic cationic groups can interact with anionic ink particles, which favors improved printing quality.[13]

There are a number of methods to synthesize H-PVA by a series of reactions of the hydroxyl groups, such as esterification, etherification, and transesterification.[14–16] Yahya et al.[17] grafted PVA with acid chlorides of long-chain fatty acids to form ester linkages. Wang and Ye[18] incorporated glycidyl-*N*-octyl-*N,N*-dimethylammonium chloride into the polymer backbone to yield H-PVA with cationic functional groups. Jialanella and Piirma[19] reported that poly(vinyl alcohol-*co*-vinyl gallate) was synthesized by a transesterification reaction between PVA and methyl-3,4,5-trihydroxybenzoate (methyl gallate). However, to the best of our knowledge, these methods are limited in the solution processing, by which only low-dimension PVA products could be yielded. Moreover, the dissolving and drying processes are a great waste of energy and time. Besides, the apparent viscosity of PVA solution would increase gradually and finally it would become a gel over time, which greatly limits the storage stability of PVA solution product. Therefore, it is still necessary to explore a more versatile and economical approach to prepare H-PVA.
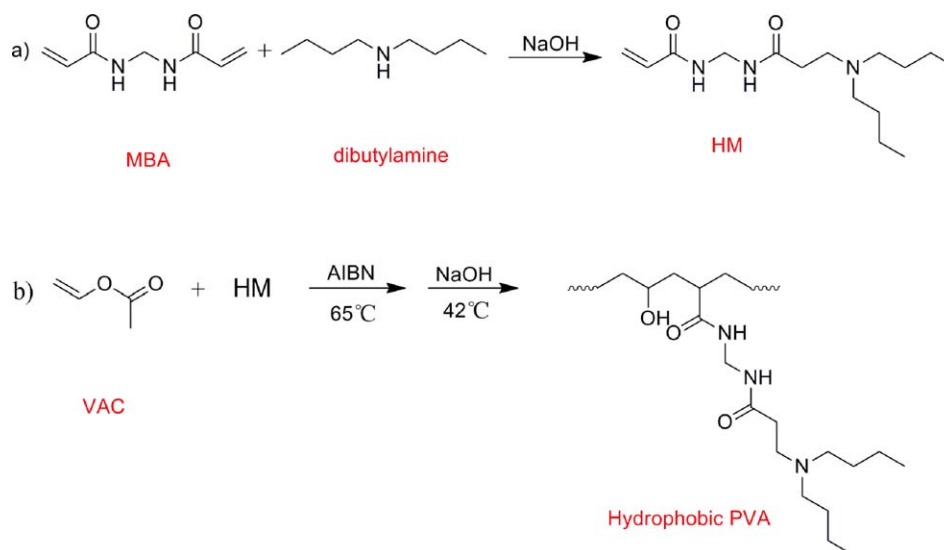
Scheme 1. Synthesis pathways of HM and H-PVA. [Color figure can be viewed in the online issue, which is available at wileyonlinelibrary.com.]

Fortunately, copolymerization of vinyl acetate (VAc) with suitable comonomers can almost solve these problems easily. This approach is conducted by directly synthesizing the H-PVA by radical solution copolymerization of VAc with a hydrophobic monomer (HM) without a dissolving and drying process, which can greatly reduce the consumption of energy. Besides, this one-step process would shorten the reaction time, simplify the operational process, and lower the cost compared with the other methods. In addition, the product is solid, which is favorable for storage and transportation. Lightly branched PVA, which could be an excellent fluid-loss additive, was prepared directly by common radical copolymerization of VAc with a bifunctional monomer allyl methacrylate (AMA) followed by saponification.[20] But the chemical structure of hydrophobic groups bonded by esters is unstable and even lost in the process of hydrolysis because of cleavage of the ester linkage.[21,22] Thus, in this work, a novel double alkyl-substituted monomer, the amide bond of which is stable and would not be lost in the hydrolysis reaction,[23] was prepared from the Michael addition reaction between dibutylamine and N,N-methylenebisacrylamide (MBA). Then the H-PVA was prepared by radical solution copolymerization of VAc with the HM and followed by an alcoholysis reaction in alkaline conditions. The synthesis pathways of the HM and H-PVA are shown in Scheme 1. Furthermore, the structures and properties of the H-PVA were investigated in detail.

EXPERIMENTAL

Materials

VAc (Sichuan Vinylon Works, China, 99.0%) was washed with an aqueous solution of $NaHSO_3$ and water, then dried over anhydrous $CaCl_2$, and finally distilled under reduced pressure. Azobisisobutyronitrile (AIBN) (Tianjing Kermel Chemical Reagents, China, 99.0%) was recrystallized in methanol. N,N-methylenebisacrylamide (MBA) (Sinopharm Chemical Reagent Co., China, 99.9%), dibutylamine (Sinopharm Chemical Reagent Co., China, 99.9%), sodium hydroxide (NaOH) (Sinopharm Chemical Reagent Co., China, 99.9%), and methanol (Sichuan Vinylon Works, China, 99.9%) were of analytical grade and used directly without further purification. The water used in the whole experiment was deionized.

Preparation of HM

The HM was prepared by the Michael addition reaction of dibutylamine and N,N-methylenebisacrylamide (MBA). In order to prevent both double bonds of MBA from being additive, excess MBA was added into the reaction system. The reaction was carried out at 30°C in a 500 mL three-necked round-bottom flask under reflux. To this, 15.4 g of MBA and 300 mL of methanol were added with agitation to make a homogeneous solution. Then 6.45 g of dibutylamine and 0.2 g of NaOH were dissolved into 40 mL methanol and added dropwise to the mixture. The molar ratio between MBA and dibutylamine was 2:1. After reacting for 4 h, the mixture was cooled and then dried in a rotary evaporator to remove the

Table I. Parameters for Solution Polymerization

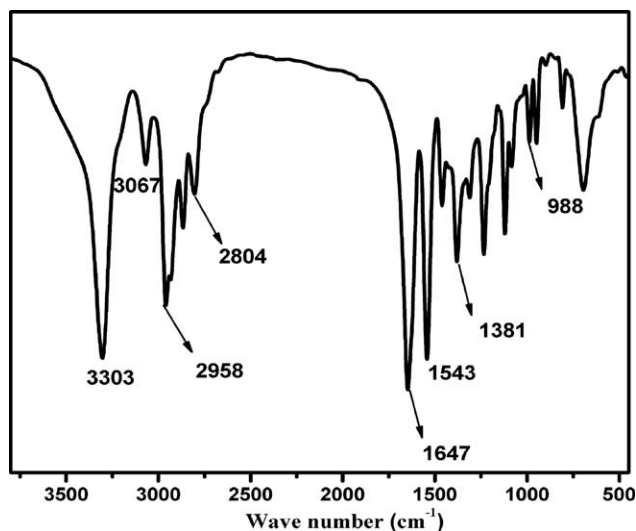| Samples	VAc (g)	HM (g)	AIBN (mg)	Methanol (g)	Conversion (%)
PVA-0	100	0	100	25	78.5
PVA-1	99	1	100	25	65.2
PVA-2	98	2	100	25	49.5
PVA-3	97	3	100	25	43.5

Figure 1. FTIR spectrum of HM.

methanol. The product was redissolved in a saturated aqueous solution of sodium chloride and petroleum ether. The organic layer containing the monomer HM was washed with water, dried, concentrated, and then stored in the freezer.

Synthesis of H-PVA

Copolymerization of VAc and HM were carried out using a 250 mL glass reactor equipped with a reflux condenser, a stirrer, and an apparatus supplying a methanol solution of HM. In this reaction system, AIBN and methanol were used as initiator and solvent, respectively. The temperature was set at 65 °C, and the reaction time was 4 h. As HM is a more reactive monomer than VAc, the feeding-comonomer method was adopted, in which HM was continuously added to the reactor. After copolymerization, the product was distilled under reduced pressure three times to remove residual monomers, washed with a large amount of water, and then dried in vacuum oven at 50 °C for 24 h to obtain pure PVAc. The conversion rate was calculated using eq. (1):

$$\text{Conversion } (\%) = \frac{m_1}{m_0} \times 100 \qquad (1)$$

where m_0 and m_1 were the weights of system before and after reaction, respectively. The results are shown in Table I. Modified PVA was prepared by an alcoholysis reaction of the obtained PVAc. The 6 wt % NaOH methanol solution was added to the 5 wt % PVAc methanol solution with stirring at 42 °C for 2 h. The mole ratio of NaOH to VAc was 0.02. Finally the product was extracted three times with methanol and then dried under vacuum at 50 °C for 24 h. The contents of HM were 0 g, 1 g, 2 g, and 3 g, so the products were named PVA-0, PVA-1, PVA-2, and PVA-3, respectively. The detailed parameters are shown in Table I.

Characterization

Fourier transform infrared spectroscopy (FTIR) was conducted on a Nicolet 560 spectrophotometer (Madison, Wisconsin, USA), ranging from 4000 to 400 cm^{-1}. The samples were dried at 50 °C for 12 h in a vacuum oven prior to testing. The structures of HM and PVA were determined by nuclear magnetic resonance (^{1}H-NMR, Bruker AV II-400 MHZ, Switzerland) at

25 °C using DMSO-d$_6$ and tetramethylsilane as the solvent and internal standard, respectively. The molecular weight and the molecular distribution were determined by gel permeation chromatography (GPC) (270max, Malvern, UK) using ultrapure water and an aqueous solution of NaNO$_3$ as the solvent and moving phase, respectively. Differential scanning calorimetry (DSC) measurements of PVA were taken on a Netzsch 204 Phoenix differential scanning calorimeter (Germany) with sample of 7–8 mg, using nitrogen as the purge gas. For the nonisothermal crystallization, the samples were first heated from room temperature to 250 °C at a heating rate of 30 °C/min, held at 250 °C for 5 min to eliminate the prior thermal history, and then cooled down to 25 °C at a cooling rate of 10 °C/min to evaluate the crystallizing ability upon cooling. The melting properties of the samples were measured by the second heating from 25 °C to 250 °C at a heating rate of 10 °C/min. The thermal stability of the samples (about 7 mg) was investigated using a thermal degradation analysis (TGA) (TA-Q600, USA) under nitrogen from 30 °C to 600 °C at a heating rate of 10 °C/min. The tensile properties of PVA samples were determined using an Instron 5567 (USA) universal testing machine at the crosshead rate of 50 mm/min. The films of PVA of size $30 \times 4 \times 0.4$ mm^3 (length $\times$ width $\times$ thickness) were prepared. The tensile fracture surfaces of PVA were observed by a scanning electron microscope (SEM; Hitachi S-3400, Tokyo, Japan) at a 20 kV accelerating voltage. Changes in the shear viscosities of the solutions were observed by a rheometer (Brookfield DV-III ULTRA, USA) over the shear rate range from 10 to 120 s^{-1}. The concentration of the solution was 4 wt %. The contact angle of the PVA films was measured by a Krüss DSA30 (Krüss, Munich, Germany) contact angle meter at room temperature. The test liquid was deionized water.

RESULTS AND DISCUSSION

Characterization of HM and H-PVA

The HM, namely N-([3-(dibutylamino)propanamido]methyl)acrylamide, was prepared by the Michael addition reaction of dibutylamine and excess MBA. The yield of this comonomer is
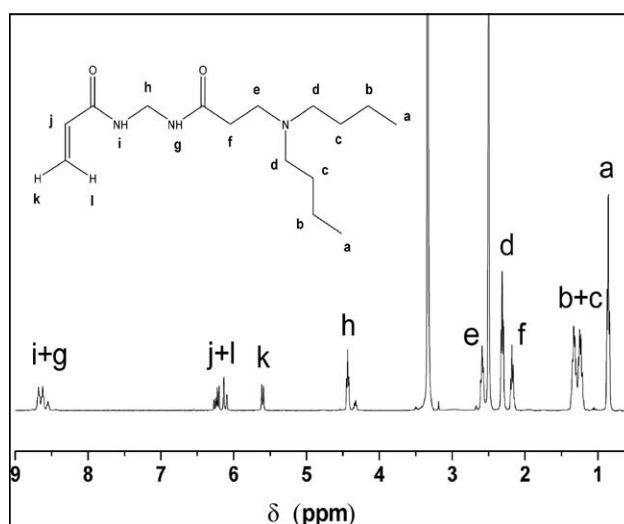

Figure 2. ^{1}H-NMR spectrum of HM.

Table II. Integration Areas of Protons of HM

H_i	H_h	H_a	H_{b+c}	H_d	H_e	H_f	H_k	H_{i+g}	H_{j+l}
Integration area S_i	1.00	2.89	4.11	2.14	1.21	1.06	0.47	0.92	1.13
Number of H_i	2	6	8	4	2	2	1	2	2

in the range of 60–78%. Figure 1 presents the FTIR spectrum of HM. The bands at the wavenumbers $3000\,cm^{-1}$ to $2804\,cm^{-1}$ (the $-CH_2$ and $-CH_3$ group stretching vibration) and $1381\,cm^{-1}$ ($-CH_3$ group bending vibration) are the obvious characteristic peaks of HM. The peaks at $3067\,cm^{-1}$, $1647\,cm^{-1}$, and $988\,cm^{-1}$ correspond to the stretching vibration of unsaturated C—H, the stretching vibration of C=C, and the bending vibration of =CH$_2$, respectively, due to the presence of the double bond (CH$_2$=C). Moreover, the absorption peaks at $3303\,cm^{-1}$, $1647\,cm^{-1}$, and $1543\,cm^{-1}$ are ascribed to the stretching vibration of the N—H group, the stretching vibration of C=O, and the bending vibration of the N—H group, respectively, confirming the existence of the amide bond.[24]

The structures of the HM are further confirmed by ^{1}H-NMR analysis. The ^{1}H-NMR spectrum (Figure 2) exhibits several characteristic peaks, such as the N—H protons (H$_g$) at 8.6 ppm, the CH$_2$=CH— region (H$_k$, H$_l$, H$_j$) at 5.5–6.3 ppm, and the methylene (H$_h$) attached to the urethane groups at 4.4 ppm. The integration area ratio of three protons at 5.5–6.3 ppm is 1:1:1, which further confirms the presence of the double bond. The triple chemical shifts at 2.1–2.6 ppm are attributed to the protons in the methylene (H$_e$, H$_d$, H$_f$) connected to the N and carbonyl groups. In addition, using the methylene protons between the two urethane groups as the internal standard, the integration areas of the protons of HM are calculated. As shown in Table II, the ratio of the integration areas of the protons is consistent with that of the number of protons. As a result, the product of HM was prepared successfully.

The H-PVA was prepared by a radical solution copolymerization of VAc with the above-prepared HM and followed by an alcoholysis reaction in alkaline conditions. The samples were dried fully in a vacuum oven prior to testing. Figure 3 shows the FTIR spectra of pure PVA and PVA-1. For pure PVA, the peaks at the wavenumbers $3326\,cm^{-1}$ (the stretching vibration peak of its side hydroxyl groups), $2940\,cm^{-1}$ (the $-CH_2$ group stretching vibration), $1139\,cm^{-1}$ (C—O crystalline stretching vibration), and $1094\,cm^{-1}$ (C—O amorphous stretching vibration) are the characteristic peaks. In the PVA-1 spectrum, the peaks observed at $1657\,cm^{-1}$ and $1551\,cm^{-1}$ are attributed to the stretching vibration of C=O and the bending vibration of the N—H groups, respectively, demonstrating that the secondary amine is successfully incorporated into the PVA. The new absorption peak at $995\,cm^{-1}$ is ascribed to the stretching vibration of C—N groups. It can also be seen that the absorption peak at $1139\,cm^{-1}$ attributed to the C—O crystalline stretching vibration in PVA slightly shifts toward the lower frequency after modification, suggesting the decrease of crystallinity in PVA,[25] and it will be further proved in the DSC analysis.

The ^{1}H-NMR spectra provide additional evidence for the successful preparation of H-PVA. As the amount of HM

incorporated into the copolymer is quite low, it is not easy to find many obvious characteristic peaks of HM. From Figure 4, in comparison with the spectrum of PVA, it can be seen that the spectrum of H-PVA shows the distinct peak at 0.85 ppm ascribed to the protons of the methyl groups (H$_l$) in the hydrophobic side chain. In addition, the very small triple chemical shifts at 2.1–2.6 ppm are attributed to the protons in the methylene (H$_g$, H$_j$, H$_k$) connected to the N, which further indicates the successful incorporation of HM comonomer into PVA.

According to the integration of the proton peak of CH$_3$COO— (S_d) and that of —OH (S_c), the degree of hydrolysis is about 99%.[26,27] Using the bands of —CH (H$_b$) and —CH$_3$ (H$_l$) as the characteristic peaks of VAc and HM, respectively, the hydrophobe content in H-PVA was calculated by the integration area according to eq. (2):

$$\text{Hydrophobe content } (\%) = \frac{S_l}{6S_c + 2S_d + S_l} \times 100\% \qquad (2)$$

where S_l S_c and S_d are the integration areas of the —CH$_3$, —OH, and CH$_3$COO— proton peaks. As shown in Table III, the actual hydrophobe content incorporated into the copolymer increases from 0.66% to 1.15% with the increasing dosage of HM in the reaction system.

The molecular weight and molecular weight distribution of the samples were determined by GPC. The results are listed in Table IV. As shown, both the number-average molecular weight (M_n) and weight-average molecular weight (M_w) decrease with the increasing amount of HM. The molecular weight distribution increases slightly from 1.8 to 2.2. This phenomenon can be explained as follows. Compared with the polymerization process of pure PVA, in addition to the chain transfer to the monomer VAc, to the macromolecular chain, and to the solvent, the chain transfer reaction to the comonomer HM exists in the
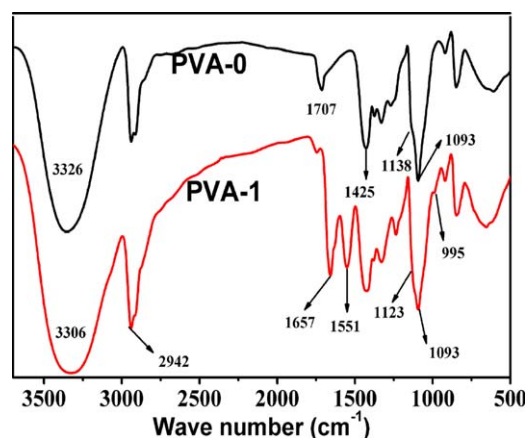

Figure 3. FTIR spectra of PVA and PVA-1. [Color figure can be viewed in the online issue, which is available at wileyonlinelibrary.com.]
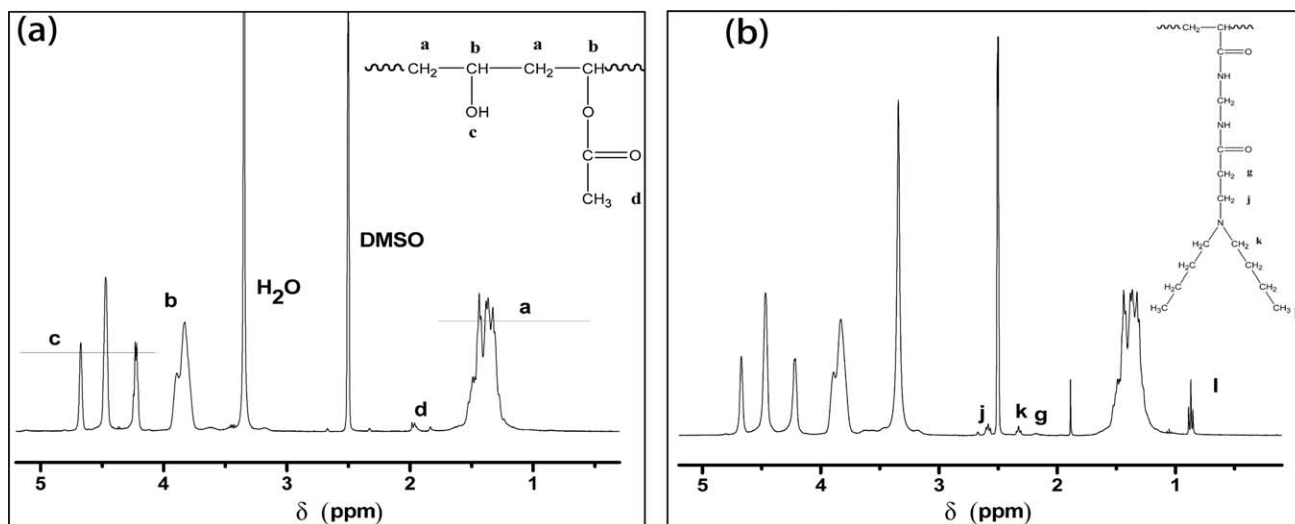
Figure 4. ^{1}H-NMR spectra of PVA and H-PVA: (a) PVA and (b) PVA-1.

Table III. ^{1}H-NMR results of PVA and H-PVA

Samples	Integration area S_c	Integration area S_d	Integration area S_g	Hydrolysis degree (%)	Mole ratio of HM unit (%)
PVA-0	1.00	0.04	—	98.7	—
PVA-1	1.00	0.03	0.03	99.0	0.49
PVA-2	1.00	0.02	0.05	99.3	0.83
PVA-3	1.00	0.02	0.07	99.3	1.15

copolymerization, which makes the molecular weight decrease and the molecular weight distribution widen. The H-PVA of relatively low molecular weight and good chemical stability shows great benefits in different industrial applications such as thickener, oil-displacement agent, and fluid-loss additive.[14,28,29]

Thermal Property Analysis

Figure 5 shows the DSC curves of PVA and H-PVA with various HM contents. The melting peaks shown in the DSC heating curves present an obvious shift to lower temperature with the increase of HM content, which is in accordance with the trend of crystalline peaks in DSC cooling curves. The degree of crystallinity (X_c) was calculated based on eq. (3):

$$X_c(\%) = \frac{\Delta H_m}{\Delta H_0} \times 100 \qquad (3)$$

where ΔH_m is the measured endothermic enthalpy of melting and ΔH_0 is the theoretical melting enthalpy of 100% crystalline PVA, which has a value of 156 J/g.[5] The detailed data of the DSC analysis are summarized in Table V. As shown, the melting temperature (T_m) decreases from 224.4 °C for PVA-0 to 210.1 °C for PVA-3. Simultaneously, it can be seen that $\triangle H_m$ and X_c decline remarkably as a result of the addition of HM to PVA, which demonstrates that the crystalline structure of PVA is destroyed. The phenomenon that the crystalline peaks become weaker and shift obviously to a lower temperature after the introduction of hydrophobic comonomer also indicates the

decrease of crystallization ability with increasing HM content. This could be explained as that the HM segments built into the copolymer destroy the regular arrangement of molecular chains and subsequently inhibit the crystallization of PVA to some extent.

The TGA curves of the pure PVA and H-PVA samples under nitrogen atmosphere are shown in Figure 6. As can be seen, the thermal decomposition temperature of H-PVA has increased by about 50 °C compared with that of pure PVA. The most probable reason is that the introduced HM unit has a shielding effect for adjacent hydroxyl removal, so the dehydration reaction between hydroxyls is less likely to happen. Therefore, the decrease of T_m and the significant increase of decomposition temperature with the increasing amount of HM lead to the acquisition of a thermal processing window, which is beneficial

Table IV. Average Molecular Weight and Molecular Weight Distribution Index of PVA and H-PVA

Samples	M_n ($\times 10^{-4}$)	M_w ($\times 10^{-4}$)	M_w/M_n
PVA-0	14.0	25.6	1.8
PVA-1	8.7	12.9	1.5
PVA-2	2.2	4.6	2.1
PVA-3	2.1	4.6	2.2

Figure 5. DSC curves of PVA and H-PVA. [Color figure can be viewed in the online issue, which is available at wileyonlinelibrary.com.]
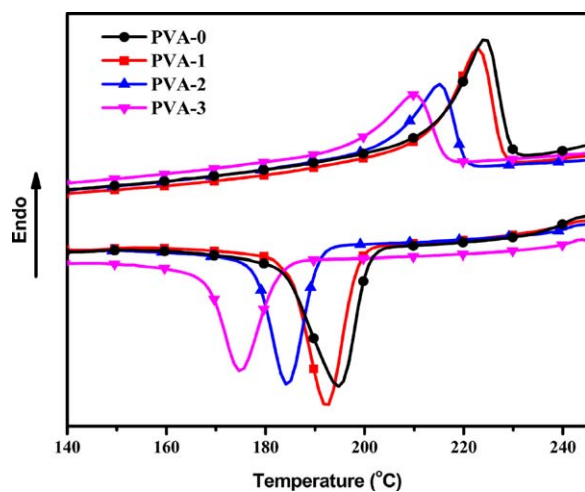

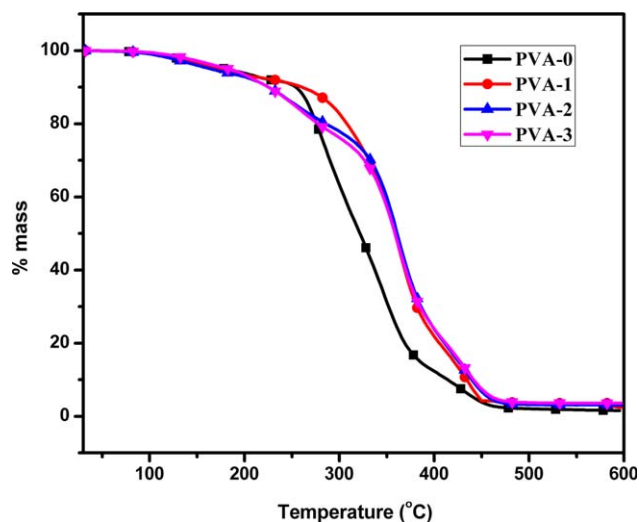**Figure 6.** TGA curves of PVA and H-PVA. [Color figure can be viewed in the online issue, which is available at wileyonlinelibrary.com.]

in realizing the thermal processing of PVA and greatly expanding its industrial application prospects.[10]

Mechanical Properties

Mechanical properties are of critical importance in practical applications. PVA films were prepared by a solution evaporation process and kept at 25 °C and 50% relative humidity for 2 days before testing. Figure 7 shows the tensile strength and elongation at break of PVA with various HM contents. It is clearly seen that the tensile strength shows a slight decrease at the lower loading level of HM, but it apparently increases as the HM content is further increased. These changes in mechanical properties can be explained as follows. On the one hand, the decrease of crystallinity and hydrogen bonds among PVA molecules would cause the decrease of tensile strength. On the other hand, these H-PVA molecules with long hydrophobic chains would help to achieve physical entanglement by intermolecular association, which would result in an increase of mechanical properties.[30,31] The H-PVA with incorporation of 1.15% HM presents a remarkable increase in tensile strength. A possible explanation is that appropriate physical entanglement of molecular chains formed by the intermolecular association of hydrophobic long chains toughens and strengthens the PVA matrix, although the hydrogen bonds between the molecular chains of PVA are weakened with the increasing amount of HM.[17] The enhancement of elongation at break with the increasing amount of HM further demonstrates the formation of physical entanglements of the hydrophobic long chains.

Morphology

The morphology of the tensile fracture surfaces of PVA is of great importance in understanding the changes in mechanical properties.[32,33] Figure 8 depicts the SEM images of the tensile fracture surfaces of (a) PVA-0, (b) PVA-1, (c) PVA-2, and (d) PVA-3. As seen from the Figure 8(a), the fracture surface of PVA-0 is very smooth and exhibits the characteristics of a typical brittle fracture. After hydrophobic modification, the tensile fracture surfaces become rough, accompanied by a large amount of stress whitening, displaying an obvious characteristic of tough fracture.[18] Furthermore, the folds and stress whitening become more and more obvious with the increasing hydrophobe content. This phenomenon can be attributed to the fact that the physical entanglement of the hydrophobic long chains could absorb much energy and hinder crack growth under a strong external shock, and at last enhance the mechanical properties of PVA.

Shear Viscosity of Solution

To investigate the intermolecular interaction in PVA and H-PVA solutions, the effect of increasing shear rate on the viscosity was measured by a rheometer at 20 °C in the shear rate range from 10 to 120 s^{-1}. The result is presented in Figure 9. It can be seen that the shear viscosity shows a decrease along with the increasing shear rate at first and gradually reaches an equilibrium value. The equilibrium viscosity of pure PVA is only 8 cps, while that of PVA-1 and PVA-2 reach 28 cps and 36 cps, respectively. The viscosity of the H-PVA solution is several times higher than that of the corresponding unmodified PVA
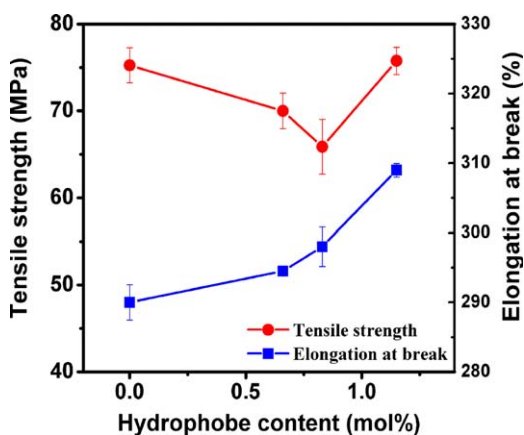
Table V. Thermal Properties and Crystallinity of PVA and H-PVA

Samples	T_m (°C)	T_c (°C)	$\triangle H_c$ (J/g)	$\triangle H_m$ (J/g)	X_c (%)
PVA-0	224.4	194.7	61.42	51.04	32.72
PVA-1	222.9	192.3	58.73	47.99	30.76
PVA-2	215.0	184.3	47.48	37.18	23.83
PVA-3	210.1	174.9	44.77	36.19	23.20

Figure 7. Tensile strength and elongation at break of PVA as a function of HM content. [Color figure can be viewed in the online issue, which is available at wileyonlinelibrary.com.]
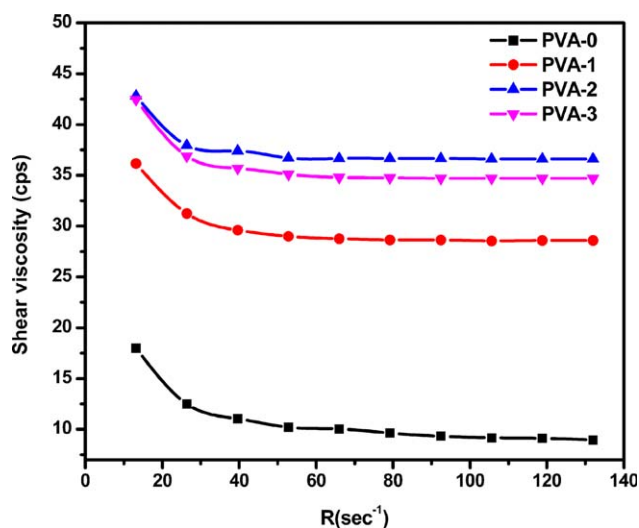

Figure 9. Shear viscosity changes of PVA and H-PVA in 4 wt % at 20 °C as a function of shear rate. [Color figure can be viewed in the online issue, which is available at wileyonlinelibrary.com.]

solution. The reason is that when a solution of PVA is subject to a shear force, the physical links are disrupted and a shear thinning behavior is observed. The much higher equilibrium viscosity of H-PVA than that of pure PVA is attributed to the stronger intermolecular forces caused by the heavy entanglement of the introduced hydrophobic long side chains and main chains.[17,19,34] The increased shear-resistance property gives it a potential application in oil chemicals.

Hydrophobic Property

The hydrophobic property can be used to enhance the water-repellent property and self-cleaning property.[35] Besides, it is of

great importance in the field of fluid-loss additives and paper-sizing agents.[11,12] The hydrophobic property was evaluated by measuring the water contact angle of the samples. When the contact angle of a water droplet on the surface of a sample is greater than 90°, it can be commonly considered as a hydrophobe.[36] The result is shown in Figure 10. The contact angle exhibits an apparently increasing trend after the hydrophobic modification. It reaches 115.0° for PVA-2 versus 55.1° for pure
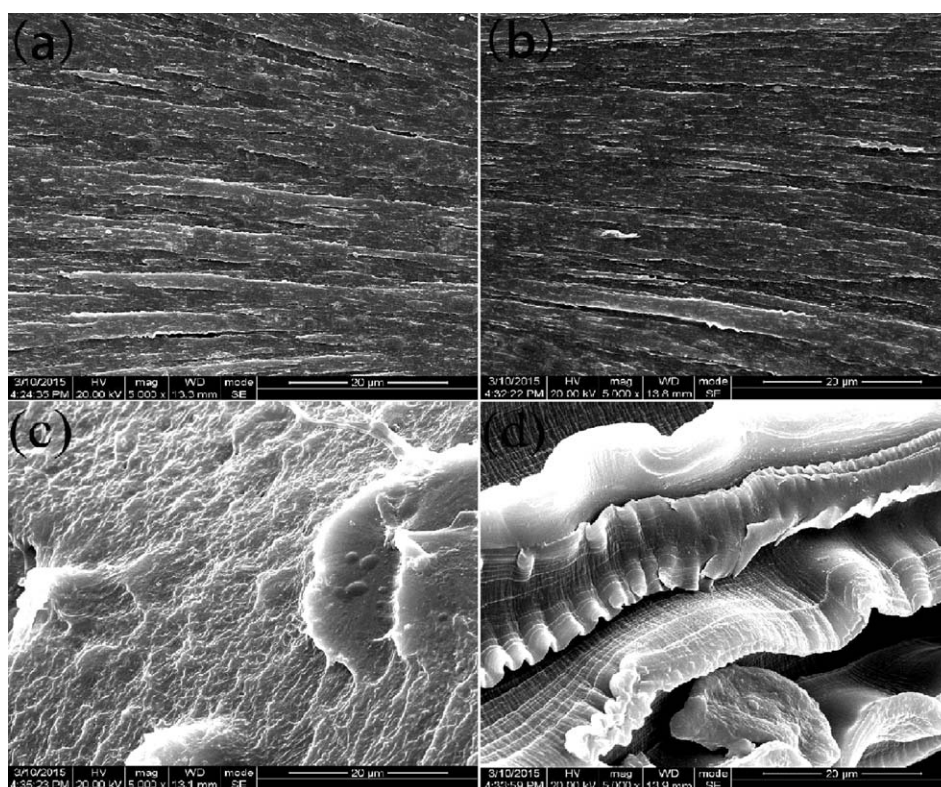

Figure 8. Morphology of the tensile fracture surfaces of (a) PVA-0, (b) PVA-1, (c) PVA-2, and (d) PVA-3.
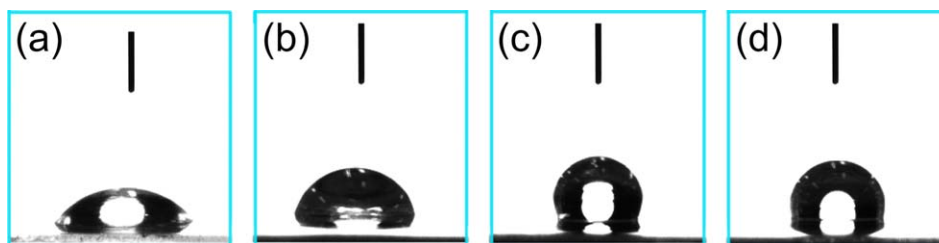
Figure 10. Contact angles of (a) PVA-0, (b) PVA-1, (c) PVA-2, and (d) PVA-3. The contact angle values are 55.1°, 80.2°, 115.0°, and 108.7°, respectively. [Color figure can be viewed in the online issue, which is available at wileyonlinelibrary.com.]
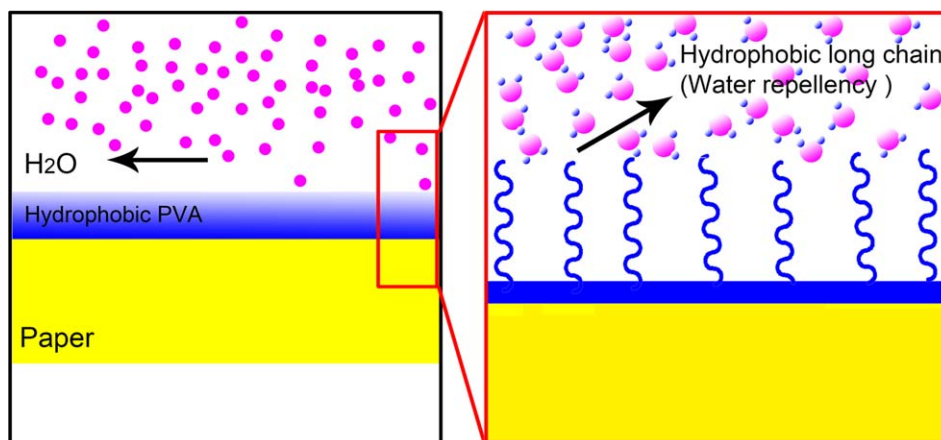

Figure 11. Schematic mechanism of the hydrophobic effect. [Color figure can be viewed in the online issue, which is available at wileyonlinelibrary. com.]

PVA, which illustrates that the hydrophobic property is largely enhanced by the copolymerization. This phenomenon is attributed to the hydrophobic nature of the long aliphatic chains distributed along the backbone and the rough surface of the PVA samples.

The mechanism of the hydrophobic effect is shown schematically in Figure 11. Generally, polymer chain ends are well known to possess a high free volume, which would bring about the surface segregation of the side chain ends because of the entropy effect.[37] When the H-PVA is applied to the paper surface or other solid surface, the long hydrophobic aliphatic chains distributed along the backbone are driven outward by the entropy effect due to the free volume of the hydrophobic side chains based on tailoring the conformational dimensions of the molecular chain, which would make the surface of the base materials extremely rough. This is beneficial for the trapping of air or gas bubbles; thus the water molecules would be pushed out from adjoining the base materials, and high water repellency is obtained.[38–41] Moreover, the hydroxyls of H-PVA show good affinity to the base materials, which could improve its adhesion strength. But with further increasing the amount of HM incorporated into the copolymer, it would be easier to form physical entanglements between the long side chains, which would cause the decrease of free volume as well as contact angle. The mechanism of the hydrophobic effect may apply to other segmented copolymers or grafted polymers.

CONCLUSIONS

A hydrophobic cation–modified PVA was prepared successfully by a radical solution copolymerization of VAc with a homemade HM. The structures of HM and H-PVA were confirmed by FTIR and ^{1}H-NMR. The mole ratios of HM units in PVA-1, PVA-2, and PVA-3 were 0.66%, 0.83% and 1.15%, respectively, which were calculated from the ^{1}H-NMR spectra. It was found that the heat-resistance and shear-resistance properties were all significantly improved, due to the incorporation of the hydrophobic long chains. The thermal decomposition temperature of H-PVA was increased by about 50 °C compared with that of pure PVA. Furthermore, the tensile strength of PVA-3 was higher than that of PVA-0, and the elongation at break showed a rising trend with increasing HM content. That is, the H-PVA became stronger and tougher with the incorporation of HM. In addition, the contact angle of PVA-2 was significantly increased up to 115.0° versus 55.1° for pure PVA, illustrating that the hydrophobic property had been greatly enhanced. This H-PVA shows great industrial application prospects in the fields of oil chemicals, paper, water-repellent coating, antifouling paint, and so on.

REFERENCES

1. Asran, A. S.; Henning, S.; Michler, G. H. *Polymer* **2010**, *51*, 868.

2. Lee, J. S.; Choi, K. H.; Ghim, H. D.; Kim, S. S.; Chun, D. *J. Appl. Polym. Sci.* **2004**, *93*, 1638.

3. Anbarasan, R.; Pandiarajaguru, R.; Prabhu, R.; Dhanalakshmi, V.; Jayalakshmi, V.; Dhanalakshmi, B.; Jayalakshmi, T. *J. Appl. Polym. Sci.* **2010**, *117*, 2059.

4. Kaboorani, A.; Riedl, B. *Compos. Part A: Appl. Sci.* **2011**, *42*, 1031.

5. Wei, L.; Ye, L. *J. Appl. Polym. Sci.* **2013**, *129*, 3757.

6. Sang, Y.; Xiao, H. *J. Colloid. Interface Sci.* **2008**, *326*, 420.

7. Addisu, G. D.; Lin, C. K.; Lee, C. K. *Appl. Mater. Interfaces* **2013**, *5*, 4745.

8. Li, H. Z.; Chen, S. C.; Wang, Y. Z. *Ind. Eng. Chem. Res.* **2014**, *53*, 17355.

9. Gacal, B. N.; Koz, B.; Gacal, B.; Kiskan, B.; Erdogan, M.; Yagci, Y. *J. Polym. Sci. Part A: Polym. Chem.* **2009**, *4*, 1317.

10. Cheng, N.; Li, L.; Wang, Q. *Plast. Rubber. Compos.* **2007**, *36*, 283.

11. Hu, Q.; Huang, G.; Zheng, J.; Su, H.; Guo, C. *J. Polym. Res.* **2012**, *19*, 1.

12. Hashem, M. M.; Kesting, W.; Hebeish, A. A.; Abou-Zeid, N. Y.; Schollmeyer, E. *Macromol. Mater. Eng.* **1996**, *241*, 149.

13. Bang, H.; Watanabe, K.; Nakashima, R.; Kai, W.; Song, K. H.; Lee, J. S.; Gopiraman, M.; Kim, I. S. *RSC Adv.* **2014**, *4*, 595718.

14. Marstokk, O.; Roots, J. *Polym. Bull.* **1999**, *42*, 527.

15. Hanna, J.; Du-Hyun, S.; In-Chul, K.; Young-Nam, K. *J. Appl. Polym. Sci.* **2015**, *132*, DOI: 10.1002/app.41712.

16. Sahoo, B.; Kandasubramanian, B. *RSC Adv.* **2014**, *4*, 22053.

17. Yahya, G. O.; Asrof, S. K.; Al-Naafa, M. A.; Hamad, E. Z. *J. Appl. Polym. Sci.* **1995**, *57*, 343.

18. Wang, J.; Ye, L. *Polym. Int.* **2012**, *61*, 571.

19. Jialanella, G.; Piirma, I. *Polym. Bull.* **1987**, *18*, 385.

20. Han, H.; Zhang, J. *J. Appl. Polym. Sci.* **2013**, *130*, 4608.

21. Moritani, T.; Yamauchi, J. *Polymer* **1998**, *39*, 559.

22. Yahya, G. O.; Ali, S.; Al-Naafa, M. A.; Hamad, E. Z. *J. Appl. Polym. Sci.* **1995**, *57*, 343.

23. Rymarczyk-Machał, M.; Zapotoczny, S.; Nowakowska, M. *J. Polym. Sci. Part A: Polym. Chem.* **2006**, *44*, 2675.

24. Ren, W.; Wu, R.; Guo, P.; Zhu, J.; Li, H.; Xu, S.; Wang, J. *J. Polym. Sci. Part A: Polym. Phys.* **2015**, *53*, 545.

25. Sun, X.; Lu, C.; Liu, Y.; Zhang, W.; Zhang, X. *Carbohydr. Polym.* **2014**, *101*, 642.

26. Gholap, S. G.; Jog, J. P.; Badiger, M. V. *Polymer* **2004**, *45*, 5863.

27. Ding, J.; Chen, S. C.; Wang, X. L.; Wang, Y. Z. *Ind. Eng. Chem. Res.* **2008**, *48*, 788.

28. Menezes, R. R.; Marques, L. N.; Campos, L. A.; Ferreira, H. S.; Santana, L. N. L.; Neves, G. A. *Appl. Clay Sci.* **2012**, 12.

29. Bauget, F.; Langevinb, D.; Lenormanda, R. *J. Colloid Interface Sci.* **2001**, *11*, 501.

30. Lin, J. S.; Chen, L.; Liu, Y.; Wang, Y. Z. *J. Appl. Polym. Sci.* **2012**, *125*, 3517.

31. Maryam, H.; Ahmad, M.; Mehran, G.; Mahmood, M. *J. Appl. Polym. Sci.* **2013**, *128*, 1640.

32. Dave, V.; Tamagno, M.; Focher, B.; Marsano, E. *Macromolecules* **1995**, *28*, 3531.

33. Nam, S. Y.; Lee, Y. M. *J. Membr. Sci.* **1997**, *135*, 161.

34. Laura, M. G.; Alejandro, J. M.; Philippe, M.; Lionel, C. *Colloids Surf. A* **2008**, *330*, 168.

35. Neinhuis, C.; Barthlott, W. *Nucleic Acids Res.* **1997**, *79*, 667.

36. Bin, H.; Yingying, L.; Qiongtao, H.; Guoliang, L.; Jian, L.; Liping, C.; Haipeng, Y. *Mater. Des.* **2015**, *84*, 277.

37. Kaya, T.; Motoko, K.; Masaru, K.; Takashi, N. *Langmuir* **2015**, *31*, 209.

38. Nadine, T.; Nadége, F.; Kateryna, F.; Jean-Marc, V.; Fabienne, P. E. *J. Phys. Chem. C* **2012**, *116*, 12599.

39. Quere, D. *Rep. Prog. Phys.* **2005**, *68*, 2495.

40. Beatríz, G.; Javier, S. P.; Roser, G. C.; Jordi, H.; Ramon, A.; Fernando, N.; Josep, S.; Félix, B.; Daniel, R. M. *Appl. Mater. Interfaces* **2014**, *6*, 17616.

41. Yi, Y.; Chen, Z.; Ming, T.; Zhongjie, D.; Jianguo, M. *J. Phys. Chem. C* **2015**, *119*, 20957.